Received: 31 July 2023 | Revised: 25 November 2023 | Accepted: 28 November 2023

DOI: 10.1111/ejn.16234

SPECIAL ISSUE ARTICLE

DOPAMINE: From Release and Modulation to Brain Diseases

EJN European Journal of Neuroscience FENS WILEY

A dual-omics approach on the effects of fibroblast growth factor-2 (FGF-2) on ventral tegmental area dopaminergic neurons in response to alcohol consumption in mice

Leonie Hose[1,2] | **Alina Katharina Langenhagen**[1,3] | **Ekaterini Kefalakes**[1] | **Theresa Schweitzer**[4,5] | **Sabrina Kubinski**[1] | **Segev Barak**[6] | **Andreas Pich**[4,5] | **Claudia Grothe**[1,2]

[1]Hannover Medical School, Institute of Neuroanatomy and Cell Biology, Hannover, Germany

[2]Center for Systems Neuroscience (ZSN), Hannover, Germany

[3]Department of Veterinary Pathology, Freie Universität Berlin, Berlin, Germany

[4]Institute of Toxicology, Hannover, Germany

[5]Core Facility Proteomics, Institute of Toxicology, Hannover, Germany

[6]School of Psychological Sciences, Tel Aviv University, Tel Aviv, Israel

Correspondence
Claudia Grothe, Hannover Medical School, Institute of Neuroanatomy and Cell Biology, OE 4140, Carl-Neuberg-Str. 1, 30625 Hannover, Germany.
Email: grothe.claudia@mh-hannover.de

Funding information
This work was funded by Deutsche Forschungsgemeinschaft (DFG) [GR 857/29-1 to CG] and Israel Science Foundation (ISF) [GR 508/20 to SB].

Edited by: Yoland Smith

Abstract

Harmful alcohol consumption is a major socioeconomic burden to the health system, as it can be the cause of mortality of heavy alcohol drinkers. The dopaminergic (DAergic) system is thought to play an important role in the pathogenesis of alcohol drinking behaviour; however, its exact role remains elusive. Fibroblast growth factor 2 (FGF-2), a neurotrophic factor, associated with both the DAergic system and alcohol consumption, may play an important role in DAergic neuroadaptations during alcohol abuse. Within this study, we aimed to clarify the role of endogenous FGF-2 on the DAergic system and whether there is a possible link to alcohol consumption. We found that lack of FGF-2 reduces the alcohol intake of mice. Transcriptome analysis of DAergic neurons revealed that FGF-2 knockout (FGF-2 KO) shifts the molecular fingerprint of midbrain dopaminergic (mDA) neurons to DA subtypes of the ventral tegmental area (VTA). In line with this, proteomic changes predominantly appear also in the VTA. Interestingly, these changes led to an altered regulation of the FGF-2 signalling cascades and DAergic pathways in a region-specific manner, which was only marginally affected by voluntary alcohol consumption. Thus, lack of FGF-2 not only affects the gene expression but also the proteome of specific brain regions of mDA neurons. Our study provides new insights into the neuroadaptations of the DAergic system during alcohol abuse and, therefore, comprises novel targets for future pharmacological interventions.

Abbreviations: DAergic, dopaminergic; DAT, dopamine transporter; DDC, dopa decarboxylase; DMS, dorsomedial striatum; ERK, extracellular signal-regulated kinase; FGF-2, fibroblast growth factor 2; FGFR, fibroblast growth factor receptor; HA, hemagglutinin; HMW, high molecular weight; IA2BC, intermittent access to 20% alcohol in a two-bottle choice; IP, immunoprecipitation; IPA, ingenuity pathway analysis; JAK, Janus kinase; KO, knockout; LMW, low molecular weight; MAPK, mitogen-activated protein kinase; MB, midbrain; mDA, midbrain dopaminergic; NAc, nucleus accumbens; PI3K, phosphatidylinositol-3-kinase; PKA, protein kinase A; PKB, protein kinase B; PLC, phospholipase C gamma; SNpc, substantia nigra pars compacta; STAT, signal transducer and activator of transcription; TH, tyrosine hydroxylase; VTA, ventral tegmental area.

Leonie Hose and Alina Katharina Langenhagen contributed equally.

KEYWORDS
alcohol addiction, alcoholism, brain reward system, dopamine receptors, FGF

1 | INTRODUCTION

Fibroblast growth factor 2 (FGF-2), also known as basic fibroblast growth factor, belongs to the FGF family comprising 22 members (Ornitz & Itoh, 2022). FGF-2 binds to all four FGF receptors (FGFRs), leading to the activation of downstream signalling pathways that are crucial for proper brain development (Ford-Perriss et al., 2001; Reuss, & von Bohlen und Halbach, O., 2003), neurogenesis (Wagner et al., 1999) and regenerative plasticity (Gómez-Pinilla et al., 1995). Apart from this, FGF-2 is essential for the development of midbrain dopaminergic (mDA) neurons (Timmer et al., 2007) and the formation of the nigrostriatal pathway in mice (Baron et al., 2012). It was previously shown that knockout of FGF-2 (FGF-2 KO) is associated with a developmental hyperplasia of mDA neurons in the substantia nigra pars compacta (SNpc) (Ratzka et al., 2012) and increased striatal volume (Rumpel et al., 2016) implying that FGF-2 KO might alter the circuitry of the projection targets of the midbrain.

mDA neurons are located in three distinct brain regions, the retrorubral field (A8), the SNpc (A9), or the ventral tegmental area (VTA, A10) and project to more distant regions of the brain (Cardoso & Lévesque, 2020; Carlsson et al., 1962; Dahlstroem & Fuxe, 1964). This classification is based on their anatomical location, cellular morphology and the area of innervation (Anderegg et al., 2015; Roeper, 2013). A common feature of all mDA neurons is the expression of the enzymes tyrosine hydroxylase (TH) and dopa decarboxylase (DDC), which are involved in the synthesis and degradation of dopamine (Björklund & Dunnett, 2007a, 2007b). Interestingly, recent works on single-cell gene profiling identified several mDA neuron subsets that, apart from their anatomical classification, also differ in their gene expression and, hence, their function (Poulin et al., 2014; Tiklová et al., 2019).

Dopamine is an important neurotransmitter in the brain, controlling voluntary movement, cognition, memory and reward (Baik, 2020). Accordingly, it is not surprising that abnormal DA transmission is associated with various neuropsychiatric disorders including Parkinson's disease, schizophrenia and anxiety disorder (Björklund & Dunnett, 2007b; Ungless & Grace, 2012). Moreover, there is growing evidence that the DA system is involved in alcohol drinking behaviour as it has been shown that mDA neurons are susceptible to alcohol-induced biochemical neuroadaptations (Morel et al., 2019) that, in turn, could promote the transition of controlled to chronic alcohol consumption. In line with this is the finding that FGF-2 is a positive regulator of alcohol drinking behaviour (Even-Chen et al., 2017). Specifically, alcohol consumption was shown to increase *Fgf-2* mRNA expression in a time-dependent and region-specific manner, and the manipulation of endogenous *Fgf-2* affects alcohol use (Even-Chen et al., 2017). Although FGF-2 seems to be a modulator of alcohol consumption, the exact molecular mechanisms and their underlying signalling pathways remain elusive.

Because FGF-2 has been previously described as a positive regulator of alcohol consumption (Even-Chen et al., 2017), we examined whether loss of endogenous *Fgf-2* affects drinking behaviour in mice. Indeed, we found that FGF-2 KO mice are less prone to alcohol drinking in a two-bottle choice model compared with wild-type mice. Therefore, we hypothesized that FGF-2 KO leads not only to anatomical changes in mDA neurons but also to an aberrant gene and protein expression, most likely resulting in functional differences in mDA neurons that could explain the lack of alcohol addiction in FGF-2 KO mice. Selective mDA immunoprecipitation, which allows specific enrichment and analysis of ribosomal mRNA of mDA neurons, showed that FGF-2 KO mice exhibit altered gene expression profiles compared with wild-type animals. Specifically, we found that out of 15 different DA markers, nine showed significant dysregulation, among which *Otx2* and *Vgat* are both characteristic genes of DA subpopulations of the VTA. Finally, we examined the effects of a global *Fgf-2* depletion in the proteome and selected signalling pathways within the areas of origin and innervation of mDA neurons (DMS, NAc and VTA) under physiological and alcohol drinking conditions. Surprisingly, mDA signalling in the VTA was altered in FGF-2 KO mice but remained unchanged under alcohol consumption. Thus, our findings suggest that FGF-2 affects the arrangement of mDA neurons into subpopulations and that it shifts mDA neurons towards mDA subtypes of the VTA that also show VTA-specific differences in mDA signalling. However, although FGF-2 KO mice are not susceptible towards an alcohol drinking behaviour, no change in VTA mDA signalling pathways was evident, implying that further mechanisms take place.

2 | MATERIAL AND METHODS

2.1 | Animals

All animals were bred at the central animal facility of the Hannover Medical School (Germany) and kept in

the same temperature- and humidity-controlled room on a 14-h light/10-h dark schedule and housed in open cages in groups of four to five animals with food and water available ad libitum. The hygienic status was routinely monitored in accordance with the FELASA recommendations (Mähler Convenor et al., 2014). No evidence of infectious agents was revealed, except for occasional positive tests for *Rodentibacter pneumotropica* and *Helicobacter* spp. All animal experiments were conducted in strict accordance with the German animal welfare law and were approved by the Lower Saxony State Office for Consumer Protection and Food Safety (LAVES Oldenburg, Germany, reference number 33.12-42502-04-18/2977 in accordance with the German Animal Welfare Act).

FGF-2-deficient mice (FGF-$2^{tm1Zllr}$; FGF-$2^{-/-}$) were maintained on a C57BL/6J background (Dono et al., 1998). Within this strain a mutation replaces the first exon of the *Fgf-2* gene with a neomycin expression cassette, thereby CUG and AUG start-codons of both high (HMW) and low (LMW) molecular weight FGF-2 isoforms were removed (Dono et al., 1998). C57BL/J6 wild-type (FGF-$2^{+/+}$) animals were used as controls and were generated by own breeding. Genotyping was performed as previously described (Ratzka et al., 2012).

$Rpl22^{tg/tg}$/DAT-$Cre^{cre/wt}$/FGF-$2^{-/-}$ mice and respective $Rpl22^{tg/tg}$/DAT-$Cre^{cre/wt}$/FGF-$2^{+/+}$ littermates of both sexes and the age of 40 days were generated by crossing *Fgf-2* deficient (Dono et al., 1998), DAT-Cre (Bäckman et al., 2006) and Rpl22-HA (Sanz et al., 2009) mice maintained on a C57BL/6J background. The Rpl22 mouse line is based on the expression of an HA-tagged ribosomal subunit (Rpl22-HA) in genetically defined cell populations and allows the isolation of actively translated, ribosome-bound RNA from these cells. Genotyping was performed by PCR using the following primers: Rpl22-for: GGG AGG CTT GCT GGA TAT G and Rpl22-rev: TTT CCA GAC ACA GGC TAA GTA CAC. Conditions were 94°C for 3 min, 94°C for 30 s, 64°C for 30 s, 72°C for 30 s, repeat steps 2–4 for 35 cycles, 72°C for 2 min. Generated products: Mutant at 290 bp, wild-type at 243 bp. DAT-Cre is a knock-in mouse strain that utilizes the endogenous dopamine transporter (DAT) gene to promote Cre expression in DA neurons. It is crucial to use mice displaying a heterozygous genotype for the DAT-Cre allele for subsequent analysis, because animals homozygous for the mutation show a significant reduction (47% downregulation) of DAT expression (Bäckman et al., 2006). Genotyping was performed by PCR using the following primers: DAT-Cre-com: TGG CTG TTG GTG TAA AGT G, DAT-Cre-wt-rev: GGA CAG GGA CAT GGT TGA CT, and DAT-Cre-tg-rev: CCA AAA GAC GGC AAT ATG GT. Conditions were 94°C for 3 min, 94°C for 30 s, 62°C for 1 min, 72°C for 1 min, repeat steps 2–4 for 35 cycles, 72°C for 2 min. Generated products: Mutant at 152 bp, wild-type at 264 bp.

2.2 | Experimental overview

Both the alcohol drinking experiment and the proteomic approach were performed using FGF-2-deficient mice (FGF-$2^{tm1Zllr}$; FGF-$2^{-/-}$). For an overview, see graphical abstract upper (behavioural assessment) and lower (proteomic analysis) third. Results generated by the use of these mice can be found in Figures 1, 3, 4 and 5 as well as Table S1.

Experiments to investigate the role of endogenous FGF-2 specifically in mDAergic neurons were performed using $Rpl22^{tg/tg}$/DAT-$Cre^{cre/wt}$/FGF-$2^{-/-}$ mice and respective $Rpl22^{tg/tg}$/DAT-$Cre^{cre/wt}$/FGF-$2^{+/+}$ littermates. For an overview, see graphical abstract middle (transcriptomic analysis) third. Results generated by the use of these mice can be found in Figure 2 as well as Tables S2, S3 and S4 and Figures S1 and S2.

2.3 | Intermittent access to 20% (v/v) alcohol in a two-bottle choice (IA2BC)

For all alcohol drinking sessions, ethanol was provided in 50-mL tubes at 11:00 am. Ethanol (absolute) was purchased from Mallinckrodt Baker, Inc. (Philipsburg, NJ, USA) and was diluted to a final concentration of 20% (v/v) with tap water. After 1 week of habituation for single housing, FGF-$2^{+/+}$ and FGF-$2^{-/-}$ mice at an age of 7 weeks were trained to consume 20% (v/v) alcohol in the IA2BC procedure as previously described (Carnicella et al., 2014). Briefly, mice of the alcohol group ($n = 5$) had three 24-h sessions of free access to two bottles per week [one with tap water and one with 20% (v/v) alcohol] on Mondays, Wednesdays and Fridays. Concurrently, animals of the control group ($n = 10$) had unlimited access to two bottles filled with tap water. During the withdrawal periods, all animals (alcohol and water group) had unlimited access to water (see Figure 1a). To prevent side preferences, the position (left or right) of the alcohol bottle was alternated for each alcohol drinking session. Both water and alcohol bottles were weighed before and after each drinking session, with measurements rounded to the nearest 0.01 g and normalized to the weekly measured body weight of each animal. Spillage of alcohol and water was measured separately and subtracted from individual fluid intakes. The preference for ethanol over water was calculated by expressing the ethanol intake as a percentage of the total liquid intake.

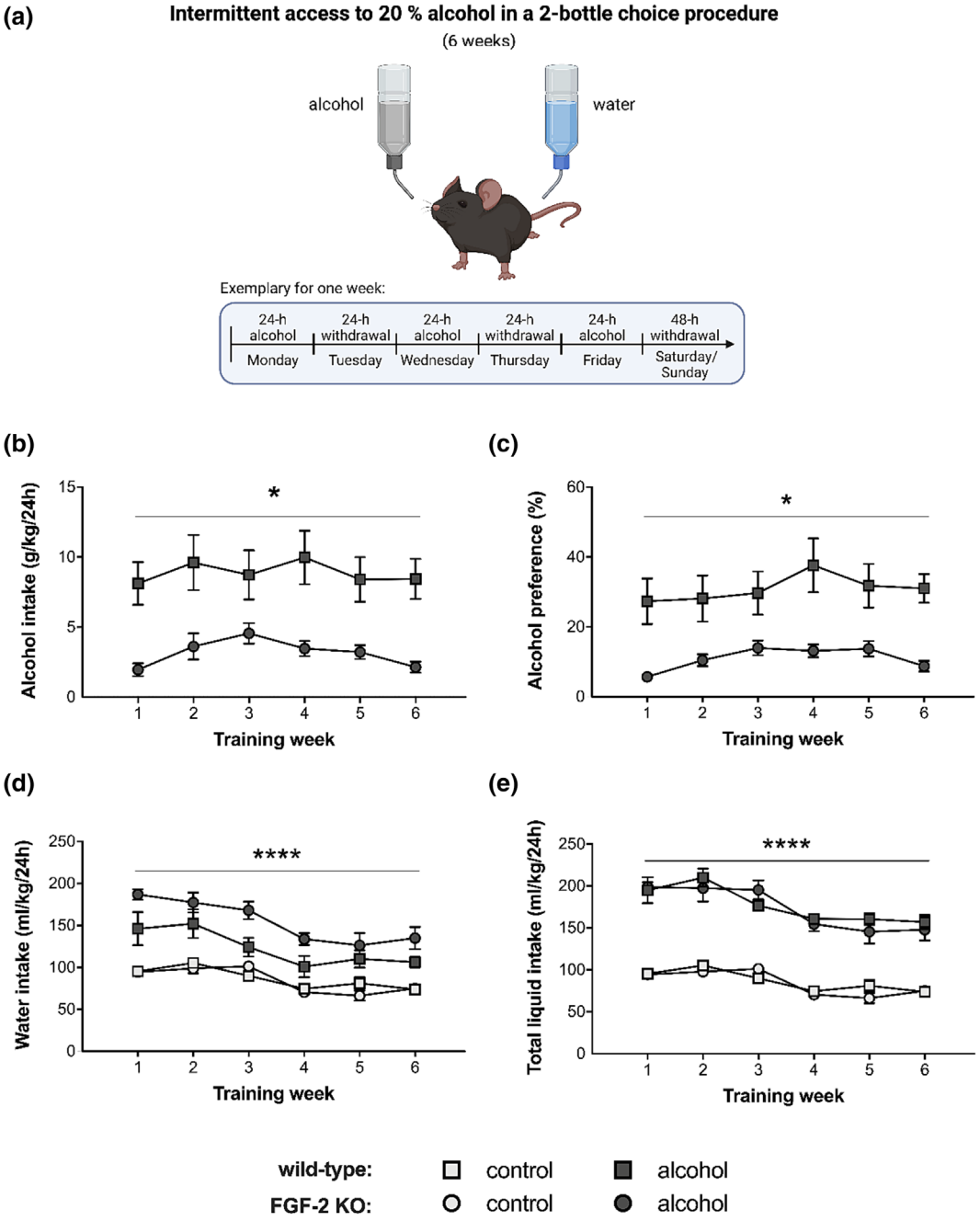

FIGURE 1 Reduced alcohol consumption in FGF-2 KO mice compared with wild-type animals. Experimental timeline of the IA2BC (intermittent access to 20% alcohol in a two-bottle choice) procedure. FGF-2 KO and wild-type mice were trained to consume alcohol over a 6-week period (a). Intake levels of alcohol (g/kg/24 h) (b) and water (mL/kg/24 h) (d) were measured in FGF-2 KO and wild-type mice. Alcohol preference (c) was calculated by dividing the amount of alcohol consumption by total liquid intake. Total liquid intake (mL/kg/24 h) was measured over 6 weeks (e). Data are presented as mean ± SEM (standard error of the mean) ($n = 5$ biological replicates for FGF-2 KO mice and $n = 10$ biological replicates for wild-type mice, respectively), two-way mixed-model ANOVA, $^{*}p \leq 0.05$, $^{****}p \leq 0.0001$.

After 6 weeks of alcohol consumption, mice at the age of 90–100 days were euthanized 48 h after the last drinking session (11:00 am), brains were isolated and different brain regions of interest were dissected (see below). Data (animal number, age, weight and experimental group) of euthanized mice are listed in Table S1.

2.4 | Tissue processing and protein digestion

FGF-$2^{+/+}$ ($n = 5$) and FGF-$2^{-/-}$ ($n = 5$) mice at the age of 90–100 days were euthanized for brain retrieval. After cervical dislocation, VTA, NAc and DMS were dissected,

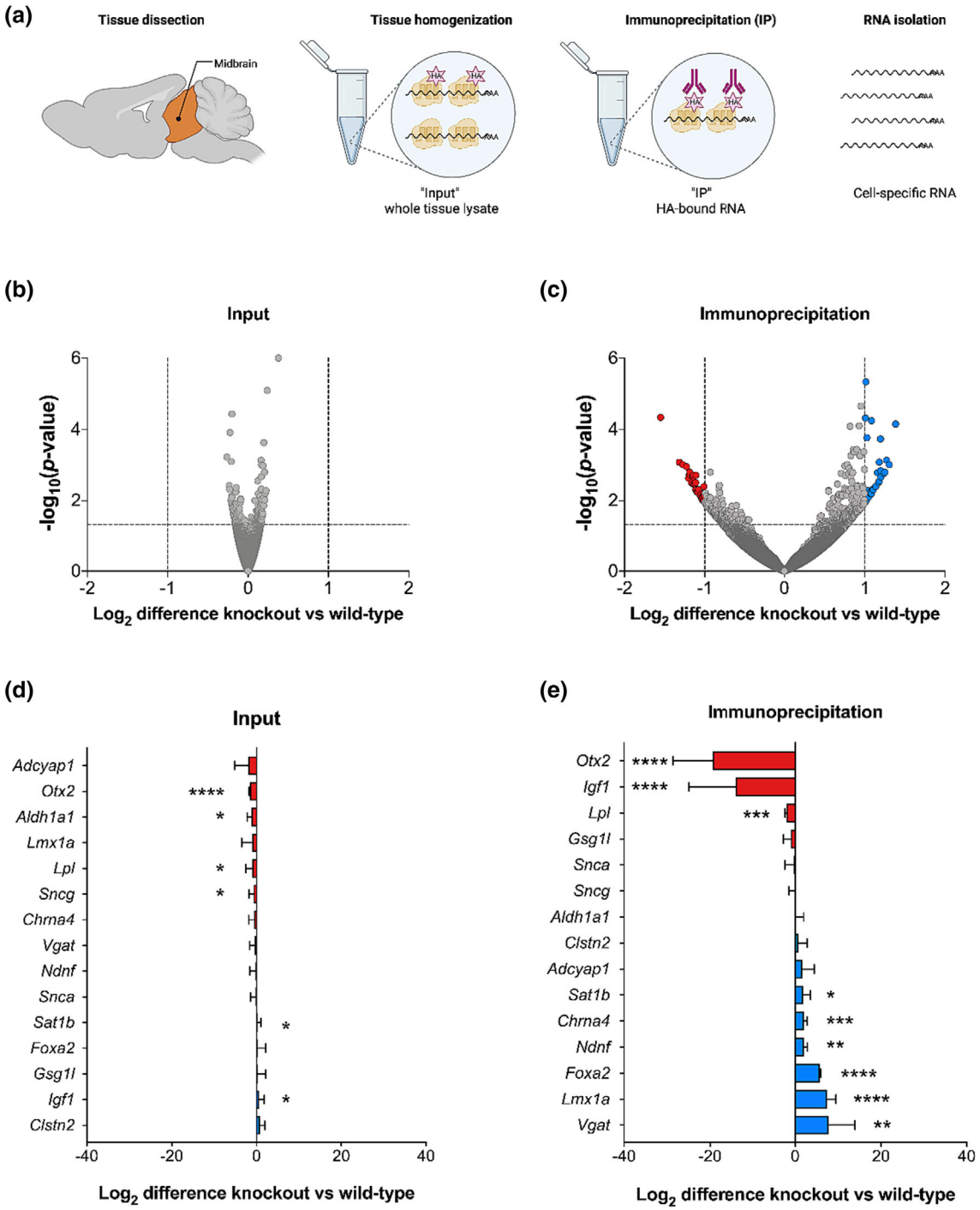

FIGURE 2 FGF-2 KO mice showed altered gene expression of mDA neuron subtype marker genes. Overview of experimental strategy for the isolation of DA neuron-specific ribosomal RNAs from midbrains of Rpl22-DAT-Cre$^{+/-}$ mice (a). Volcano plots illustrate differentially expressed mRNA (dot) in FGF-2 KO mice compared with wild-type littermates in input (b), representing whole midbrain mRNA and immunoprecipitation (c), representing mRNA specifically derived from DAergic neurons. Each dot displays a measured mRNA. Dotted lines indicate the minimal regulation factor (Log_2 difference >1; <−1) and the significance level $-\log_{10}$ (0.05), red dots: minimum twofold significant downregulation, grey dots: no regulation, blue dots: minimum twofold significant upregulation. The expression of marker genes characteristic for different subpopulations of mDA neurons according to Poulin et al. (2014) was analysed by qRT-PCR. The analysis was performed on input RNA (i.e., whole midbrain RNA) (d) and RNA specifically derived from mDA neurons (e). Enriched genes of FGF-2 KO mice in comparison with their wild-type littermates are represented in blue and de-enriched genes in red. Data are presented as mean ± SEM ($n = 3$, referring to three pull-down experiments, with pooled samples adding up to $n = 6$ animals) analysed with two-way ANOVA, *$p \leq 0.05$, **$p \leq 0.01$, ***$p \leq 0.001$, ****$p \leq 0.0001$.

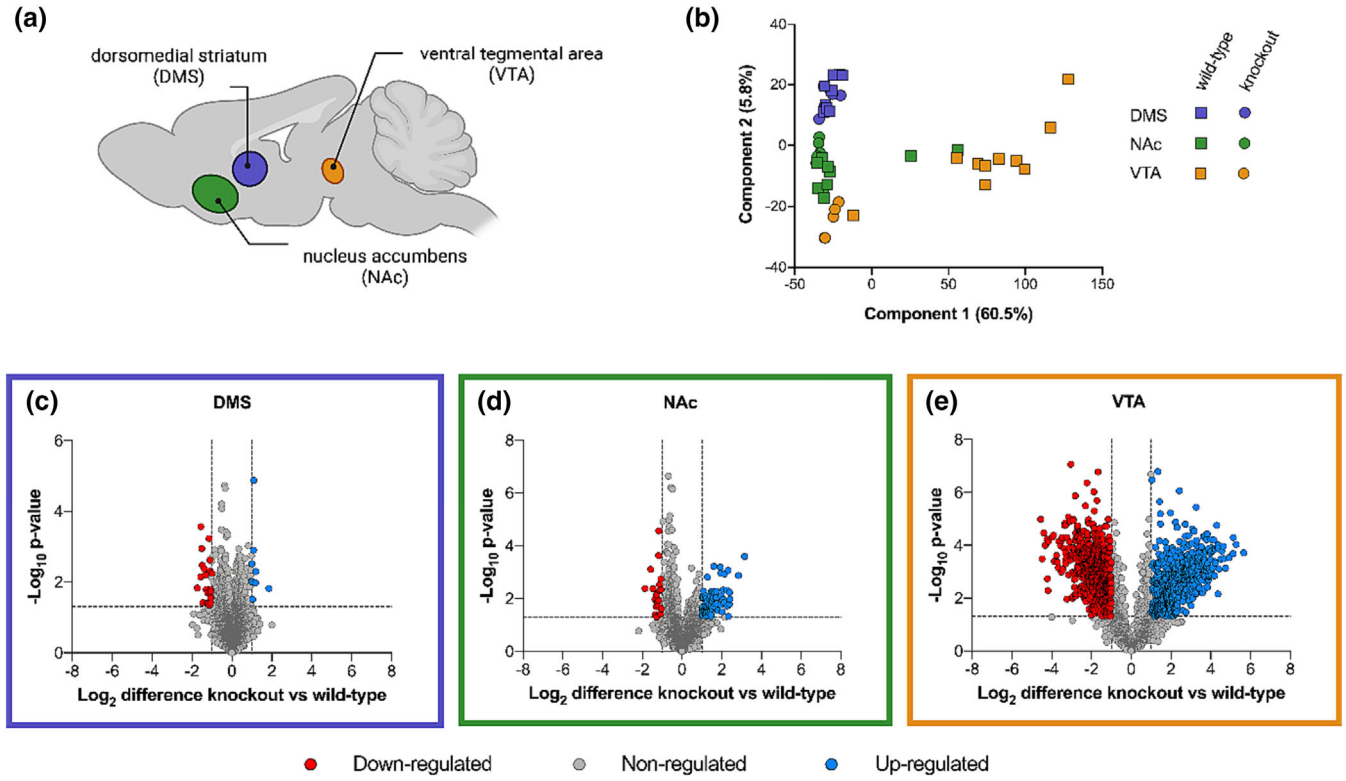

FIGURE 3 Higher differences in the VTA-specific proteome of FGF-2 KO mice. (a) Brain regions investigated by proteomics analysis. (b) Principal component analysis (PCA) of significantly altered proteins ($p \leq 0.05$) in the DMS (purple), NAc (green) and VTA (orange) of both FGF-2 knockout and wild-type mice. Volcano plots illustrate differentially expressed proteins due to the loss of Fgf-2 in DMS (c), NAc (d) and VTA (e). Dotted lines indicate the minimal regulation factor (Log_2 difference >1; <−1) and the significance level $-\log_{10}$ (0.05), red dots: twofold significant downregulation, grey dots: no regulation, blue dots: twofold significant upregulation.

snap-frozen in liquid nitrogen and stored at −80°C until further use. Frozen tissues were mechanically homogenized with syringe and cannula (first 20 G followed by 25 G), and extraction of total protein was performed using the AllPrep DNA/RNA/Protein Mini Kit (QIAGEN GmbH, Hilden, Germany) in accordance with the manufacturer's instruction. Total protein concentration was measured photometrically at 540 nm using Pierce™ BCA Protein Assay Reagent (Thermo Fisher Scientific, Waltham, Massachusetts, USA). Protein separation and tryptic digestion were performed as described before (Junemann et al., 2017). In brief, 100-µg protein lysate was heated at 95°C for 5 min and alkylated at room temperature by adding 40% acrylamide for 30 min. Protein separation was done on 4%–20% precast gels (BioRad, Hercules, California, USA) by electrophoresis. Gels were fixed and stained with Page Blue Protein staining solution (Thermo Fisher Scientific), and each lane was divided into three equal-sized fractions. Then, each fraction was manually cut into 1-mm^3 pieces. Gel pieces were destained by adding twice 50% ACN/50 mM ammonium bicarbonate (ABC) followed by dehydration with 100% ACN and vacuum centrifugation. Rehydration of gel pieces on ice followed for 60 min with 10% ACN/20 mM ABC containing 10 ng/µL trypsin (Promega, Madison, WI, USA). Digestion proceeded overnight at 37°C and 350 rpm and was terminated by adding 200 µL 50% ACN/0.5% TFA. Extraction of peptides followed by adding 100 µL 50% ACN/0.2% TFA and completed by adding 100 µL ACN for 30 min. Supernatants were pooled and dried by vacuum centrifugation.

2.5 | LC–MS analysis

Dried peptides were solved in 2% ACN/0.1% TFA and separated via reverse phase chromatography using a nanoflow system (RSLC, Thermo Fisher Scientific) based on their hydrophobicity. Peptides were first loaded onto an Acclaim PepMap™ precolumn (75 µm id, 2-cm length, 3-µm C18 particle size, 100-Å pore size, Thermo Fisher Scientific) and separated on a 50-cm µPAC™ column (Thermo Fisher Scientific). Peptides were separated by a 120-min binary gradient with varying concentrations of eluant A (0.1% formic acid, FA) and eluant B (80% ACN, 0.1% FA) and a constant flow rate of 0.5 µL. The

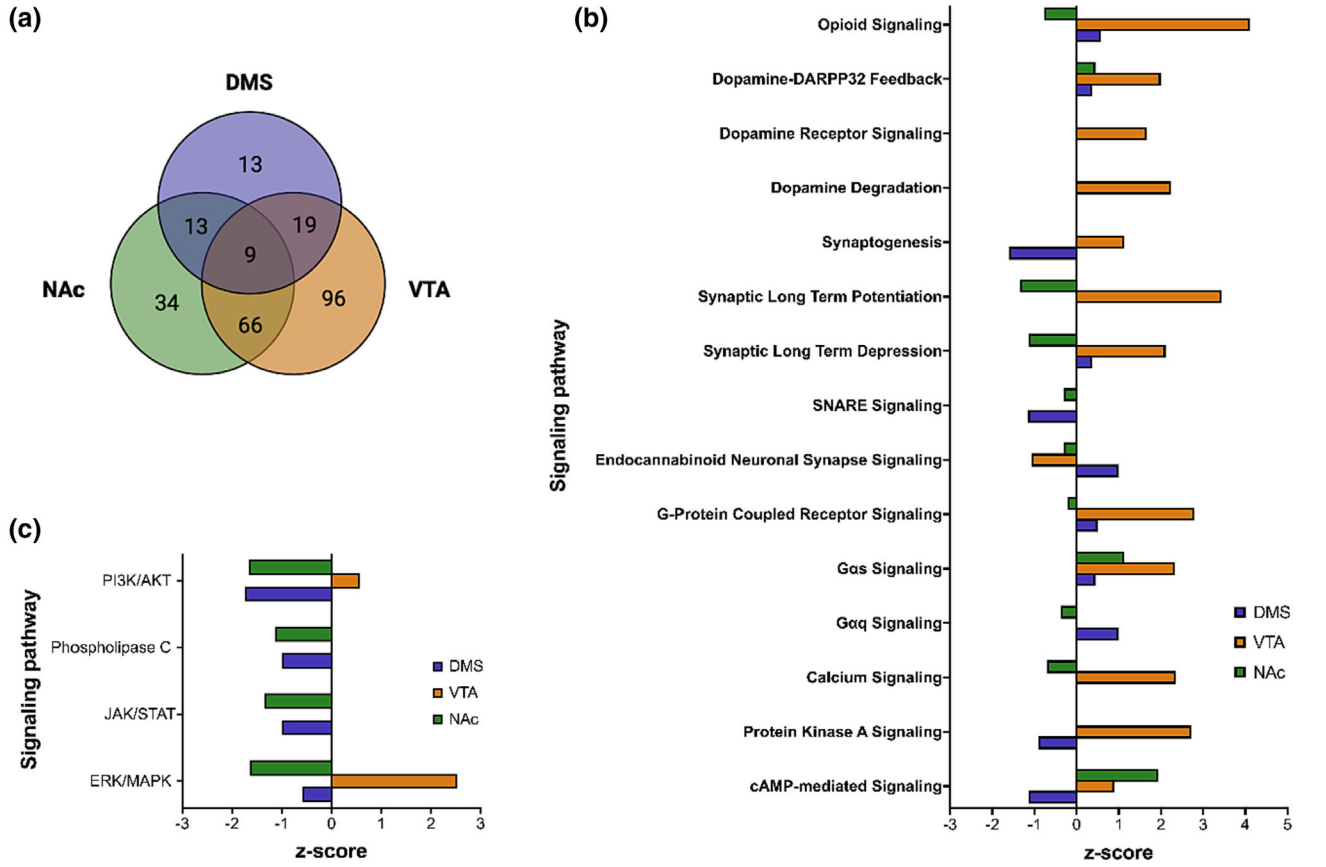

FIGURE 4 Signalling pathways significantly altered by Fgf-2 deficiency. Total numbers of significantly regulated signalling pathways by the loss of Fgf-2 in the DMS (purple), NAc (green) and VTA (orange) (a). IPA™ pathway analysis of significantly activated proteins ($p < 0.05$) shows regulation of several dopamine and synaptic pathways (b) or FGF-2 signalling pathways (c).

gradient started with 4% eluant B for 3 min and increased to 25% within the following hour. Hydrophobic peptides were eluted by increasing B to 95% within further 32 min. This was held for 4 min and re-equilibration was performed by decreasing B back to 2.5% within a minute where it was held for further 15 min. Mass spectra were acquired with an Orbitrap Exploris 240 system and a Top-30 method was used. For MS1 scans, the resolution was set to 60,000 and the range 350–1900 m/z was scanned. A normalized AGC target of 300% and a minimum injection time of 5000 were set. MS2 scans were acquired with a resolution of 15,000 following HCD fragmentation at 30% normalized collision energy. The first mass was set to 110 m/z, time to 100 ms and the normalized AGC target to 100%.

2.6 | Data processing for proteomics approach

Raw proteomics data were processed with MaxQuant software (version 1.6.17.0) using the Andromeda search engine (Cox & Mann, 2008). Spectra were searched against the Swiss-Prot reviewed *Mus musculus* UniprotKB database (version 09/2021). Propionamidation of cysteine was set as fixed modification, whereas oxidation of methionine, N-terminal acetylation and deamidation of glutamine and asparagine were set as variable modifications. The second peptide search was activated. The false discovery rate was set to 0.01 on protein and peptide level, and a maximum of two missed cleavages was allowed. Only proteins that were quantified in at least 70% of the samples were used for further data processing. Differences in protein abundance resulting from varying protein loads were normalized by subtracting the median intensity of each sample. Data evaluation and analysis were performed using Perseus (Version 2.0.6.0) and Microsoft Excel. Data visualization was done using GraphPad Prism 8 (GraphPad, San Diego, CA, USA). Analysis of canonical pathways was conducted using ingenuity pathway analysis (IPA; QIAGEN GmbH, https://digitalinsights.qiagen.com/, access: 8 November 2022). IPA software predicts regulatory proteins by comparing upregulated and downregulated proteins to a hand-curated database. For IPA analysis, all significantly altered proteins were used ($p \leq 0.05$).

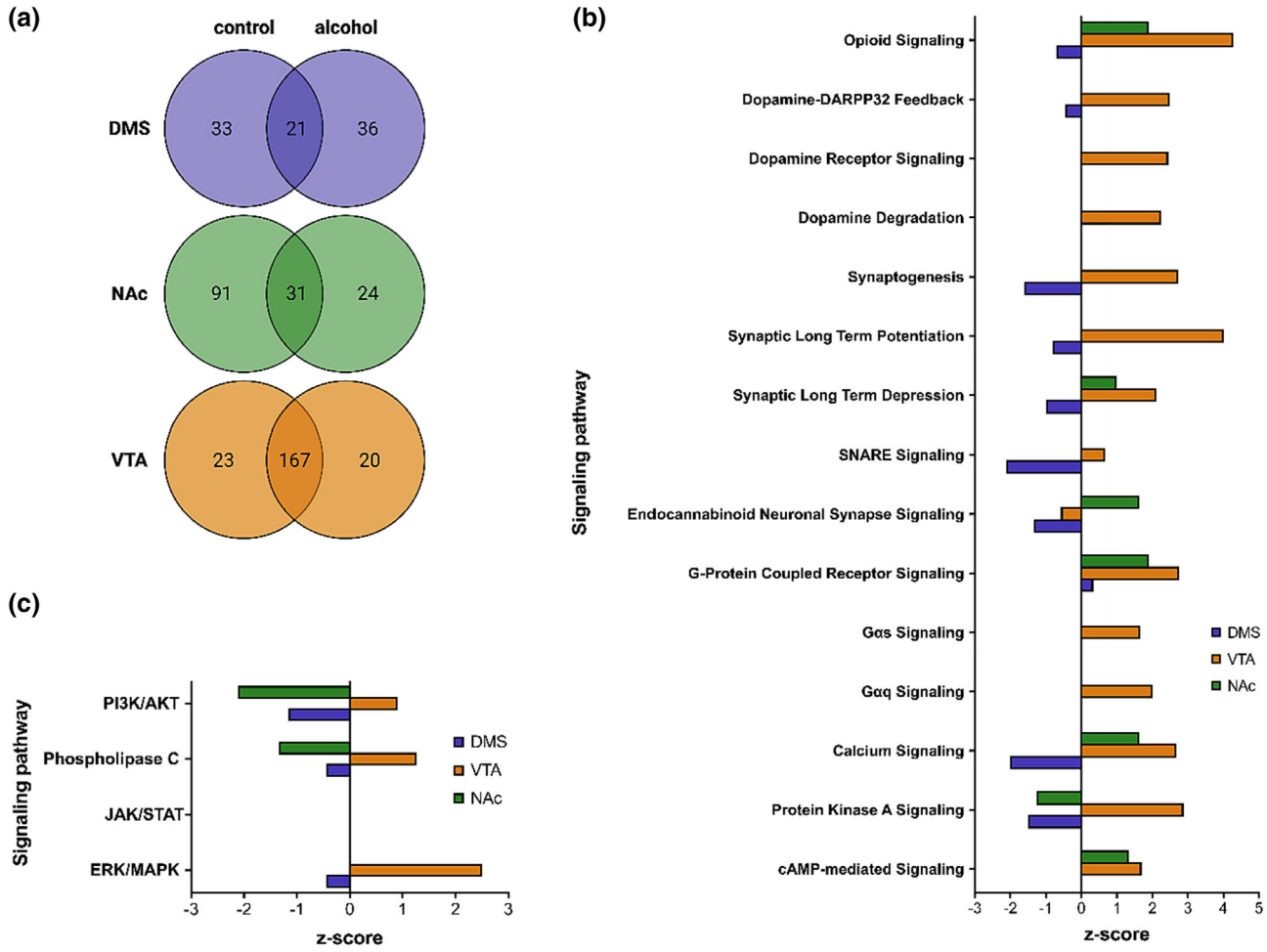

FIGURE 5 Alcohol-induced activation/deactivation of signalling pathways. Total numbers of significantly regulated signalling pathways in the alcohol group compared with control groups in the DMS (purple), NAc (green) and VTA (orange) (a). IPA™ pathway analysis of significant proteins ($p < 0.05$) shows regulation of several pathways comprising either dopamine and synaptic pathways (b) or FGF-2 signalling pathways (c).

2.7 | Immunoprecipitation of polyribosomes and cDNA synthesis

Mice were euthanized by cervical dislocation. Whole midbrains (MBs) (cerebellum and hemispheres were removed, bregma: −2.30 mm = rostral border, bregma −4.04 mm = caudal border) of Rpl22$^{+/-}$/DAT-Cre$^{+/-}$/FGF-2$^{-/-}$ and respective Rpl22$^{+/-}$/DAT-Cre$^{+/-}$/FGF-2$^{+/+}$ animals ($n = 6$) were carefully dissected, immediately frozen in liquid nitrogen and stored at −80°C until further use. MBs were processed by immunoprecipitation as described by Sanz et al. (2009). Ribosomal mRNA complexes were isolated from lysates of pooled samples (two animals per sample) by using RNeasy® Micro Kit (50) (QIAGEN, Cat. #74034). Utilizing Ovation® RNA-Seq System V2 amplification of the whole transcriptome and preparation of complementary DNA (cDNA) was achieved (see below). To confirm the enrichment of RNA from DAergic neurons, *tyrosine hydroxylase* (*Th*) and *Dat* expressions were analysed by qRT-PCR (see below). Results showed an enrichment of about 30- to 40-fold for *Th* and about 20-fold for *Dat* compared with input. 1–3 µg cDNA were used for transcriptomics by the Research Core Unit Genomics (RCUG) of the Hannover Medical School for library preparation and sequencing (Illumina NextSeq 550). cDNA was also used for qRT-PCR analysis to analyse markers of specific subtypes of DAergic neurons.

2.8 | cDNA synthesis and quantitative RT-PCR

A total amount of 1-µg RNA was converted to cDNA using the iScriptTM cDNA Synthesis Kit according to the manual (Bio-Rad, Cat. #170-8891). RNA quantification

was performed by the Nanodrop system (Epoch, Bio Tek®). For quantitative real-time PCR, 10-ng cDNA was mixed with 0.3-μL primer mix (10 μM each forward and reverse primer) and 7.5-μL POWER SYBR® Green PCR Master Mix (Applied Biosystems, Cat. #4367659) added up to 15 μL per reaction. Primer sequences and melting points of PCR products are listed in Tables S2 and S3. Samples were run in triplicates. qRT-PCR was performed in 96-well plates using the StepOnePlusTM instrument and corresponding software (Applied Biosystems, Inc., Foster City, CA, USA). The thermal cycling protocol was as follows: initial denaturation for 10 min at 95°C, 40 cycles of amplification with 15 s at 95°C, followed by 1 min at 60°C. Finally, a melting curve was calculated for each well to ensure the specificity of the PCR product. Fold changes in mRNA level compared with the wild-type littermates were calculated using the $2^{-\Delta\Delta Ct}$ method and normalized to the reference gene (*Gapdh*). The enrichment score is given as a ratio of immunoprecipitated mRNA (IP) divided by whole tissue homogenate (Input).

2.9 | Library preparation, sequencing and raw data processing

From all cDNA samples, 3 μL was used for shearing. This corresponds to approximately 300–500 ng of DNA (on average 450 ng). Shearing was performed in a Covaris S220 in microTUBE AFA Fibre Snap-Cap Tubes (PN 520045) in the S-Series Holder microTUBE (PN 500114). The shear parameters were according to the manufacturer's instructions (https://www.covaris.com/wp/wp-content/uploads/resources_pdf/pn_010368.pdf) for the production of fragments with a size of 150–200 bp (peak incident power: 175 W; duty factor: 10%; cycles per burst: 200; time: 300 s). After purification using Agencourt Ampure Beads, fragment libraries were prepared in half-reaction batches starting with 100 ng of fragmented DNA using the NEBNext® Ultra™ II DNA Library Prep Kit for Illumina® (Illumina, #E7645) according to the manufacturer's instructions. Libraries were barcoded by a dual indexing approach. Fragment length distribution of individual libraries was monitored using Bioanalyzer High Sensitivity DNA Assay (Agilent Technologies, Cat. 5067-4626). Quantification of libraries was performed by use of the Qubit® dsDNA HS Assay Kit (ThermoFisher Scientific, Q32854). Equal molar amounts of individually barcoded libraries were pooled for a common sequencing run in which each library constituted 8.3% of overall flowcell/run capacity. The library pool was denatured with NaOH and was finally diluted to 1.8 pM according to the Denature and Dilute Libraries Guide (Document # 15048776 v02; Illumina). 1.3 mL of the denatured pool was loaded on an Illumina NextSeq 550 sequencer using a Mid Output Flowcell (130 M cluster) (Illumina, Cat. 20024904). Sequencing was performed with the following settings: Sequence reads 1 and 2 with 76 bases each; Index reads 1 and 2 with 8 bases each. 10% of PhiX was added to the sequencing reaction. BCL files were converted to FASTQ files using bcl2fastq Conversion Software (Illumina, version v2.20.0.42). The FASTQ files were adapted, and quality trimmed using Trim Galore! (Version 0.4.1) with default settings as described in the User Guide except for the setting of the quality cutoff (-q/--quality), which was set to a Phred score of 15. Trim Galore! used Cutadapt (version 1.9.1) as subroutine. Quality control of FASTQ files was performed by FastQC (version 0.11.4) before and after trimming. After trimming, FASTQ files were mapped against a reference genome with the splice-aware aligner STAR (version 2.5.0c) to generate BAM files. The BAM files were built in a 2-pass Mapping (--twopassMode Basic) and were finally sorted (--outSAMtype BAM SortedByCoordinate). All other settings have been left as default as described in the manual. The genome index files were created by STAR with default settings using *Mus musculus* sequence and annotation data (UCSC, build mm10) available on illumina's iGenome site (http://support.illumina.com/sequencing/sequencing_software/igenome.html). The average number of reads entering the mapping process across all analysed samples was 12.2 million. The average percentage of uniquely mapped reads was 78.2% of reads mapped to multiple loci was 4.4%, and of unmapped reads was 17.4%. Normalization and differential expression analysis was performed with DESeq2 (Galaxy Tool, version 2.11.40.2) with default settings except for 'Output normalized counts table', which was set to 'Yes'.

2.10 | Statistics

All statistical analyses were performed using GraphPad Prism 8 (GraphPad, San Diego, CA, USA). Alcohol intake and preference were analysed with two-way mixed-model ANOVA with a between-subjects factor for the genotype (FGF-$2^{+/+}$, FGF-$2^{-/-}$) and a within-subjects factor for the training week. Water and total liquid intake were analysed using a three-way mixed-model ANOVA with genotype and treatment group (alcohol, water) as between-subject factors, and a within-subjects factor for the training week. ANOVA was followed by Fisher LSD post hoc analysis. In all cases, differences were considered significant when $p \leq 0.05$ and were represented as follows: $^{*}p \leq 0.05$, $^{**}p \leq 0.01$, $^{***}p \leq 0.001$, $^{****}p \leq 0.0001$.

3 | RESULTS

3.1 | FGF-2 KO mice exhibit reduced alcohol intake levels

FGF-2 was shown to positively regulate the alcohol drinking behaviour of mice (Even-Chen et al., 2017). Thus, we first investigated whether FGF-2 KO affects alcohol intake levels of mice. Therefore, intermittent access to 20% alcohol in a two-bottle choice (IA2BC) procedure was used (Carnicella et al., 2014). In this drinking experiment, FGF-2 KO and wild-type mice were trained to consume 20% alcohol voluntarily over a 6-week period (Figure 1a).

We found that FGF-2 KO mice consumed lower amounts of alcohol and showed a reduced alcohol preference compared to wild-type animals (Figure 1b–c). The reduced alcohol intake of FGF-2 KO mice was accompanied by an increased water intake compared to wild-type animals (Figure 1d). Moreover, animals of the alcohol group exhibited higher intake levels of water and total liquid (Figure 1d–e). Taken together, our results suggest that loss of FGF-2 reduces the voluntary alcohol consumption, whereas increases the water consumption of mice.

3.2 | Validation of DA markers reveals mDA-specific isolation via Ribotag-mediated immunoprecipitation (IP)

It was previously shown that loss of *Fgf-2* gene was associated with 35% more mDAergic neurons located in the ventral midbrain of mice (Ratzka et al., 2012). Thus, to investigate the functional impact of a *Fgf-2* ablation on the mDAergic system, the ribosomal transcriptome of FGF-2 KO animals was examined. mDAergic neurons were selectively exploited by RiboTag technology, as this method is based on Cre recombinase-induced expression of hemagglutinin (HA)-Tag fused to ribosomal protein L22 (Rpl22) (Sanz et al., 2009). By crossing Rpl22-HA mice with DAT-Cre$^{+/-}$ mice, expressing Cre recombinase driven by the DAergic neuron-specific DAT promoter, wild-type exon 4 is deleted and replaced by HA-tagged exon 4 specifically in cells expressing Cre recombinase. Consequently, Rpl22-DAT-Cre$^{+/-}$ mice were obtained expressing HA-tagged ribosomes specifically in mDA neurons (Figure S1). Whole midbrain tissues of those mice were extracted and homogenized. From the tissue lysate, HA-tagged ribosomes were pulled down using anti-HA antibody and immunoprecipitated (IP) RNA was sequenced (Figure 2a).

By qRT-PCR, we confirmed the enrichment of genes specific for DAergic neurons (e.g., *Dat*, *Th* and *Girk2*), whereas markers for excitatory neurons (e.g., *Vglut1* and *Slc1a1*), inhibitory neurons (*Cck*, *Slc32a1*, *Sst*, *Gad1* and *Calb2*), astrocytic (*Gfap*), and oligodendrocytic (*Cnp1*) genes were less present, shown as log fold change between HA-IP RNA and total RNA (Figure S1b). These data demonstrate that the use of Rpl22 provides high specificity towards DAergic neuron retrieval.

3.3 | Altered gene expression in mDA neurons in FGF-2 KO mice

Next, we aimed to elucidate whether FGF-2 KO and wild-type mice show mDA-specific differences on a transcriptome level. We, therefore, conducted transcriptome analysis using Rpl22-DAT-Cre FGF-2 KO mice, whereas Rpl22-DAT-Cre FGF-2 wild-type mice were used as controls. Whole midbrains were dissected, and RNA sequencing of mDAergic neuron HA-Tag enriched mRNA (IP) was performed. In order to get deeper insights into the effect of FGF-2 KO on gene expression patterns of mDAergic neurons, we performed RNA-sequencing (RNA-Seq).

RNA-Seq analysis revealed a good correlation between biological replicates (Figure S2a–d) and strong enrichment of DAergic markers, whereas markers specific for glial cells, excitatory and inhibitory neurons (Figure S2e) were less abundant in the RNA samples isolated by RiboTag approach compared with the input samples. Although no differentially expressed genes were detected in the input samples (Figure 2b), IP samples revealed a clear difference in the transcriptome of mDA neurons in FGF-2 KO mice (Figure 2c). A total of 32 genes showed a significantly higher gene expression in FGF-2 KO animals compared with the wild-type littermates and 29 genes revealed lower gene expression. Table S4 lists 10 genes showing significantly higher and lower expression patterns, respectively. Taken together, these results demonstrate that FGF-2 KO leads to an altered transcriptome specifically in DAergic neurons.

3.4 | FGF-2 KO results in a potential shift towards VTA-specific mDA neuron subpopulations

mDA neurons consist of subsets of functionally and genetically defined cell populations (Bodea & Blaess, 2015; La Manno et al., 2016; Poulin et al., 2014; Tiklová et al., 2019). Briefly, Poulin et al. demonstrated that single-cell sequencing allows the identification of six different subpopulations of DAergic neurons, which are distinguished by their unique gene expression pattern (Poulin et al., 2014). In order to examine the potential

role of FGF-2 in cell fate commitment of some of these neuronal subpopulations, the expression of marker genes characteristic for different subpopulations of mDA neurons was analysed. Therefore, both input RNA (representing whole midbrain RNA) and IP RNA (representing actively translated RNA) were retrieved by mDA neuron-specific IP of wild-type and FGF-2 KO mice.

Validation by qRT-PCR analysis demonstrated significant changes in the expression of several subtype-specific markers (Figure 2c–d). In input samples, a significantly higher expression of *Igf1* was found, whereas *Otx2*, *Aldh1a1*, *Lpl* and *Sncg* were lower expressed in FGF-2 KO animals compared with their wild-type littermates (Figure 2d). IP samples, containing only RNA from mDA neurons, showed stronger differences than input samples in FGF-2 KO animals compared with wild-type mice (Figure 2e). Specifically, *Vgat*, *Lmx1a*, *Foxa2*, *Ndnf*, *Chrna4* and *Sat1b* were significantly higher expressed, whereas *Otx2*, *Igf1* and *Lpl* were significantly lower expressed in FGF-2 KO mice compared with their wild-type littermates (Figure 2e). Thus, analysis of the FGF-2 KO transcriptome shows that loss of FGF-2 leads to the dysregulation of DAergic markers towards DAergic subpopulations found in the VTA.

3.5 | Differential proteome expression of FGF-2 KO mice shows brain region-specificity

Because of the evident differences in the transcriptome of mDAergic neurons of FGF-2 KO mice (Figure 2), we examined whether loss of FGF-2 affects protein translation, too. To identify potential differences between wild-type and FGF-2 KO mice on the proteome level, an LC–MS-based approach was used. The origin and target regions of mDAergic projections, namely, NAc, DMS and VTA, were analysed (Figure 3a). For multivariate analysis, principal component analysis (PCA) revealed brain region specificity (Figure 3b). DMS is distinct from NAc and VTA, based on component 2, whereas the latter show more similarities in few samples. Interestingly, clustering of VTA retrieved samples allowed additional differentiation between FGF-2 KO and wild-type mice based on component 1 (Figure 3b).

To examine changes in the proteome of FGF-2 KO mice, their proteomic content was normalized to that proteomic content of wild-type animals. MS-based proteomic analysis revealed a total of 4658 protein groups. However, only protein groups that were quantified in at least 70% of all samples were used for further bioinformatic analysis. Only significantly regulated proteins ($p \leq 0.05$) and proteins that were altered by a factor of at least $\log_2 \pm 1.0$ were considered as regulated. Volcano plots (Figure 3c–e) depict the differentially expressed proteins that are downregulated (red), upregulated (blue) or without a significant differential expression (grey). As shown in Figure 3c–d, only minor changes were found in the DMS and NAc because of FGF-2 KO. In fact, loss of FGF-2 led to 31 significantly altered proteins in the DMS (Figure 3c) and 99 in the NAc (Figure 3d), respectively. Contrary, FGF-2 KO resulted in 1084 significantly regulated protein groups in the VTA, of which 581 were downregulated and 503 were upregulated (Figure 3e), supporting the notion that FGF-2 KO plays a crucial role in VTA-specific gene expression and subsequent protein translation.

3.6 | FGF-2 KO leads to VTA-specific alterations of DA signalling cascades

We further aimed to identify the signalling pathways of the differentially translated proteins. Therefore, all proteins that were significantly altered ($p \leq 0.05$) were analysed by the IPA™ software. IPA™ uses the generated *p*-value and z-score as statistical parameters to describe the quality of predicted events. The *p*-value includes the number of proteins involved in a signalling pathway (provided by IPA™) and the overlap of those proteins within the uploaded data. The *z*-score describes the observed regulation status. Thus, a *z*-score below 0 predicts inactivation of the signalling pathway, whereas a *z*-score greater than 0 indicates activation. In general, the higher or lower the *z*-score, the better the measured protein regulations correspond to the activation or inactivation of the corresponding signalling pathway.

The number of signalling pathways that were regulated due to the FGF-2 KO is shown in Figure 4a. A total of 122 pathways were significantly altered in the NAc, 54 in the DMS and 190 in the VTA. These pathways were either specific to one brain region or overlapping with other brain areas (Figure 4a). Figure 4b shows a selection of pathways involved in DA transmission and synaptic alterations and their regulation in FGF-2 KO mice compared with the wild-type animals. Interestingly, most signalling cascades were activated predominantly in the VTA. The pathways of the VTA showing the highest activation caused by FGF-2 KO were the opioid signalling pathway, synaptic long-term potentiation and the synaptogenesis signalling pathway (Figure 4b). Moreover, we identified significant alterations in G-protein coupled receptor signalling, cAMP-mediated signalling and protein kinase A (PKA) signalling in the VTA (Figure 4b), all of which are cascades downstream of DA binding receptors. Together, these results indicate that depletion

of FGF-2 is associated with an activation of DA signalling pathways as well as synaptic long-term potentiation, demonstrating that lack of endogenous *Fgf-2* alters the DAergic system, especially in the VTA.

Binding of FGF-2 to its main target, FGFR1, leads to the activation of several intracellular signalling pathways, including the extracellular signal-regulated kinase (ERK)/mitogen-activated protein kinase (MAPK), phosphatidylinositol-3-kinase (PI3K)/protein kinase B (PKB, also known as AKT), phospholipase C gamma (PLC) pathway and the JAK/STAT pathway (Ornitz & Itoh, 2022; Reuss, & von Bohlen und Halbach, O., 2003). Thus, we next examined if the absence of FGF-2 affects the regulation of these signalling cascades and whether this can be assigned to one of the brain regions investigated. As shown in Figure 4c, all four signalling pathways were activated in the DMS and the NAc of FGF-2 KO mice compared with wild-type mice. Interestingly, this effect was not detected in the VTA. In fact, in the VTA, the ERK/MAPK pathway was activated in the absence of FGF-2. Together, these data suggest that loss of FGF-2 affects its downstream signalling cascades in a brain region-specific manner, with a predominant deactivation occurring in the target regions of DAergic neurons (DMS and NAc), and activation of the ERK/MAPK signalling is specifically detected in the VTA.

3.7 | Alcohol consumption only marginally affects DA signalling in FGF-2 KO mice

We found that animals lacking FGF-2 consumed less alcohol compared with wild-type animals (Figure 1b). Moreover, we showed that FGF-2 KO led to dysregulations of signalling pathways (Figure 4b–c), including synaptogenesis and dopaminergic signalling, and that these signalling alterations were specific for the VTA. Additionally, we found that loss of *Fgf-2* leads to alterations in the signalling cascades downstream of FGFR1, the main receptor target of FGF-2. Next, we aimed to clarify whether alcohol consumption has an impact on the activation of these particular pathways. Therefore, the proteome of FGF-2 KO mice and wild-type animals was examined after 6 weeks of voluntary alcohol access in the two-bottle choice model.

As shown in Figure 5a, several pathways were activated in either the alcohol group, the control, or in both groups. In particular, the largest overlap with a total of 167 signalling pathways was found in the VTA, and only 23 dysregulated pathways were identified in the control group, whereas 20 showed a specific regulation in the alcohol group within this brain area (Figure 5a). In contrast, within the NAc, 91 dysregulated signalling cascades were found in the control group, 24 signalling pathways were found to be regulated in the alcohol group, and 31 signalling pathways were regulated in both groups (Figure 5a). Next, we investigated the impact of voluntary alcohol intake on the regulation of signalling pathways related to DA signalling, synaptogenesis and FGF-2 signalling, which were already activated in FGF-2 KO mice (Figure 5b–c). Interestingly, only marginal differences were found regarding the activation of DAergic pathways of VTA in the alcohol drinking group (Figure 5b). Contrarily, activation in some DA signalling pathways in the NAc was observed. Specifically, the opioid signalling pathway, synaptic long-term potentiation and depression, G-protein coupled receptor (GPCR) signalling and calcium signalling were activated by alcohol consumption (Figure 5b). Furthermore, the deactivation of some signalling pathways could be observed under alcohol conditions, including dopamine-DARPP 32 feedback signalling, synaptic long-term potentiation and depression and calcium signalling (Figure 5b). Nonetheless, we found that alcohol not only shows an FGF-2-dependent region-specific activation of DA signalling but also shows a regional activation of FGFR downstream signalling. Hence, we found that alcohol consumption abolished FGF-2-induced deactivation of JAK/STAT and ERK/MAPK signalling exclusively in the DMS and NAc (Figure 5c).

To summarize, alcohol-induced changes in proteomic signalling cascades were prominently detected in both the NAc and DMS, whereas activation of DA-associated signalling pathways of the VTA remained unaffected. These results suggest that alcohol consumption induces region-dependent molecular neuroadaptations in the signalling pathways of intracellular FGF-2 signalling (downstream of the FGFRs) and DA pathways, predominantly in NAc and DMS.

4 | DISCUSSION

Within this study, we investigated the effects induced by a loss of FGF-2 in the DAergic system and how these changes are linked to alcohol drinking behaviour. The main findings are as follows: (a) FGF-2 KO leads to reduced alcohol intake levels in the two-bottle choice mouse model over a 6-week period, (b) FGF-2 KO induces subtype-specific alterations in mDA neuron gene expression profiles, (c) FGF-2 KO is associated to the activation of mDAergic signalling pathways in the VTA and (d) voluntary alcohol consumption only marginally affects the activation of proteomic signalling cascades in the NAc and DMS of FGF-2 KO mice.

FGF-2 was first linked to alcohol consumption when mice offered a 20% alcohol choice over a 5-week period showed an increased *Fgf-2* mRNA expression in the DMS (Even-Chen et al., 2017). Moreover, *Fgf-2* mRNA expression in several murine brain regions of the same model showed that voluntary alcohol consumption leads to reduced mRNA expression of *Fgf-2* in the DMS over a period of 6 weeks (Rösner et al., 2010). Because of the changes in gene expression of *Fgf-2*, it seems that *Fgf-2* is an alcohol-responsive gene particularly altered in the DMS region (Even-Chen et al., 2017; Rösner et al., 2010). In addition to the effects of alcohol consumption on *Fgf-2* mRNA expression, manipulation of endogenous FGF-2 influenced the alcohol drinking behaviour of mice, too (Even-Chen et al., 2017). Systemic administration of recombinant FGF-2 (rFGF-2) increased alcohol consumption in mice, whereas inhibition of endogenous FGF-2 reduced alcohol intake (Even-Chen et al., 2017). Recently, it was also shown that mice lacking endogenous FGF-2 consumed lower amounts of alcohol, an alcohol-specific effect, as the intake and preference of sucrose, a natural reward, was unaffected (Even-Chen et al., 2022). These results support our present finding that FGF-2 KO mice consume less alcohol compared with wild types, manifesting FGF-2 as an important regulator of alcohol drinking behaviour in mice.

In order to examine the DAergic transcriptome, RiboTag technology developed by Sanz et al. (2009) was applied, which allows the isolation of actively translated mRNA exclusively from DAergic neurons via IP. Enrichment of DAergic marker genes in IP samples revealed high methodological reproducibility as results are in agreement with previous studies (Sanz et al., 2009). It was possible to extract mDAergic neurons from a diverse group of neuronal subgroups with different origins, innervation targets and functions (Tiklová et al., 2019). Several groups aimed to resolve the heterogeneity of mDA neurons based on cell morphology, electrophysiological properties, susceptibility and axonal projections (Björklund & Dunnett, 2007a; Cardoso & Lévesque, 2020; Roeper, 2013; Yetnikoff et al., 2014). Single-cell RNA sequencing enabled the identification of specific mDAergic subtypes defined by a unique molecular fingerprint out of which seven are commonly known in mice (Poulin et al., 2020, 2014; Saunders et al., 2018; Tiklová et al., 2019): subtype 1 ($Sox^+Aldh1a1^+$), subtype 2 ($Sox^+Aldh1a1^-$), subtype 3 ($Vglut2^+Aldh1a1^-$) located in SN pars lateralis, subtype 4 ($Vglut2^+Aldh1a1^-$) located in the VTA, subtype 5 ($Vglut2^+Vgat^+$), subtype 6 ($Vglut2^+Aldh1a1^+Otx2^+$) and subtype 7 ($Sox^+Aldh1a1^+$) (Poulin et al., 2020). Apart from them, additional subtypes are suggested (Kramer et al., 2018). Accordingly, it has been shown that mDAergic subtypes also exist in humans (La Manno et al., 2016) and partially share the aforementioned subpopulations described in mice (Agrawal & Lynskey, 2008; Kamath et al., 2022; Smajić et al., 2022). Because FGF-2 was previously found to influence the DAergic system, we aimed to elucidate the role of endogenous FGF-2 on the mDA neuron-specific gene expression. Indeed, we found that loss of FGF-2 led to altered expression of mDAergic subtype-specific marker genes. Specifically, *Otx2*, *Igf1* and *Lpl1* were significantly downregulated, whereas *Vgat*, *Lmx1a*, *Foxa2*, *Ndnf*, *Chrna4* and *Sat1b* were significantly upregulated. Interestingly, the most regulated genes *Vgat* and *Otx2* are specific for DAergic subtypes 5 and 6, respectively. Although the altered gene regulation observed might not only derive from a change in the relative ratio of mDAergic subtypes in FGF-2 KO mice but could also result from differences in expression profiles of individual neurons, our results suggest that FGF-2 KO mice comprise a higher number of subtype 5 and a lower number of subtype 6 mDA neurons. Subtype 5 neurons are localized mostly in the VTA, whereas subtype 6 neurons are found in the ventromedial VTA (Poulin et al., 2020). The former is thought to project to the lateral habenula (Garritsen et al., 2023) and display a deviant behaviour in response to reward-stimulating treatment compared with other neuron subtypes (Root et al., 2020). The latter project to the lateral septum, the medial shell of the NAc and the tubercle column (Beier et al., 2015; Lammel et al., 2008; Poulin et al., 2018). VTA neurons projecting to the medial shell of the NAc induce aversive behaviours (Brischoux et al., 2009); however, little is known about the role of DAergic subtypes in addiction and particularly alcohol dependence. Nevertheless, transcriptomic changes suggest an aberrant function and responsiveness to therapeutic agents of affected mDA neurons as the dysregulation of mDA neurons is a known cause for neuropsychiatric disorders, especially schizophrenia (Björklund & Dunnett, 2007a) and alcohol addiction (Even-Chen et al., 2017).

Consistent with our transcriptome analysis showing the impact of FGF-2 on mDA neuron cell fate specification into mDAergic subtypes, we further found that absent FGF-2 leads to an altered protein translation and activation of subsequent signalling cascades, particularly in the VTA. We found that DAergic neuron signalling pathways, like dopamine receptor signalling and DARPP32 signalling, showed significantly higher protein levels in FGF-2 KO mice compared with wild types. Although we cannot completely rule out that the VTA-related results account for the entire ventral midbrain, including the SNpc, it is indicated that this region is highly susceptible to the lack of FGF-2, reflected by the number of dysregulated proteins and downstream

signalling pathways in FGF-2 KO animals. FGF-2 is an important neurotrophic factor involved in the development and maintenance of mDAergic neurons (Grothe & Timmer, 2007; Reuss & Unsicker, 2000; Reuss, & von Bohlen und Halbach, O., 2003; Timmer et al., 2007). Using organotypic co-cultures of ventral midbrain and forebrain explants derived from embryonic wild-type and FGF-2 KO mice, it was previously shown that mDA fibre length was increased in FGF-2 KO explants compared with wild-type explants, indicating that FGF-2 induces mDA fibre outgrowth and, hence, the innervation of target areas (Baron et al., 2012). Similar use of ex vivo half-brain explants showed that loss of FGF-2 was associated with a 6.5% increase in STR volume, with no evident difference in fibre density (Rumpel et al., 2016). This increased volume was hypothesized to be related to 35% more DAergic neurons we previously found in FGF-2 KO animals specifically in the SNpc (Ratzka et al., 2012).

Recently, it was shown that FGFR1 has an equal role in alcohol consumption as FGF-2, and its mRNA expression was altered in mice exposed chronically to alcohol (Even-Chen & Barak, 2019). Similar to *Fgf-2* mRNA expression (Even-Chen et al., 2017), upregulated *Fgfr1* mRNA was found in the DMS of mice that were voluntarily offered 20% of alcohol (Even-Chen & Barak, 2019). Consistent with this, systemic administration of the FGFR1 inhibitor PD173074 or direct infusion of it into the DMS of rodents decreased alcohol intake levels and preference (Even-Chen & Barak, 2019). Because inhibition of FGFR1 itself had no effect on sucrose consumption, FGFR1-mediated effects are specifically related to alcohol consumption and not to other rewards (Even-Chen & Barak, 2019). Binding of FGF-2 to FGFR1 activates signalling cascades, including PI3K/AKT, ERK/-MAPK, JAK/STAT and the PLCy signalling pathway (Eswarakumar et al., 2005). Administration of the specific PI3K inhibitor wortmannin (Bain et al., 2003) directly in the DMS of rats decreased alcohol intake (Even-Chen & Barak, 2019), suggesting that the effects of FGF-2/FGFR1 are predominantly mediated through this signalling cascade. This observation is consistent with our results as we found a reduction of proteins related to the PI3K/AKT signalling cascade and our data indicate reduced activation of this signalling pathway within the DMS and NAc of FGF-2 KO mice. Because this signalling pathway was previously found to be involved in the FGF-2-mediated effects on drinking behaviour, our data suggest that reduced activation of this signalling cascade might be associated with the reduced drinking behaviour observed in FGF-2 KO mice. Interestingly, the loss of *Fgf-2* induces opposing effects in the FGFR1-mediated signalling cascades in NAc, DMS and VTA. All FGFR1 signalling pathways were reduced in the DMS and NAc of FGF-2 KO mice, whereas a significant activation of the ERK/MAPK signalling cascade was only observed in the VTA of these animals. The ERK/MAPK signalling cascade has already been linked to glial cell line-derived neurotrophic factor (GDNF), another regulator of alcohol consumption (Barak et al., 2015; Carnicella et al., 2008). GDNF acts as a negative regulator of alcohol intake, as infusion of it into the VTA of rats reduced ethanol self-administration (Carnicella et al., 2008). This effect was specifically to the VTA, because injection of GDNF into the SNpc did not affect alcohol intake (Carnicella et al., 2008). Moreover, GDNF reduced alcohol drinking behaviours via activation of ERK1/2 in the VTA (Liran et al., 2020), and inhibition of the ERK/MAPK signalling cascade blocked GDNF-induced decrease in alcohol self-administration (Carnicella et al., 2008). Together, these data suggest that the ERK/MAPK pathway, which was found to be increased in the VTA of FGF-2 KO mice, acts as a 'stop' pathway, as its activation leads to reduced alcohol consumption, and thus decelerates the transition from moderate to excessive alcohol consumption (Ron & Barak, 2016). Contrarily, the PI3K/AKT signalling pathway, which was decreased in FGF-2 KO mice, seems to be a 'go' pathway as it favours the transition from moderate to uncontrolled excessive alcohol consumption and dependence (Liran et al., 2020; Ron & Barak, 2016).

Overall, by analysing the transcriptome and proteome in relation to alcohol use, we examined the impact of a global FGF-2 depletion. We detected a shift in mDA subtype markers, as well as changes in the proteome and consecutive signalling pathways of several brain regions of the DAergic system. We suggest that these molecular neuroadaptations of the DAergic system are a possible cause of tolerance towards alcohol drinking. However, although the FGF-2-related changes within the DAergic system are, to a certain extent, responsible for the reduced alcohol drinking behaviour of FGF-2 KO mice, further studies are needed to elucidate the precise molecular mechanisms behind them.

AUTHOR CONTRIBUTIONS

Study concept and design: Leonie Hose, Alina Katharina Langenhagen, Andreas Pich, Segev Barak and Claudia Grothe; Design of the work: Leonie Hose and Alina Katharina Langenhagen; Animal drinking experiments: Leonie Hose; Acquisition, analysis and interpretation of the data for the work: Leonie Hose, Alina Katharina Langenhagen, Theresa Schweitzer and Andreas Pich; Statistics: Leonie Hose, Alina Katharina Langenhagen and Theresa Schweitzer; Writing the original draft: Leonie Hose, Alina Katharina Langenhagen and Ekaterini Kefalakes; Writing—critical revisions/editing: Leonie

Hose, Alina Katharina Langenhagen, Ekaterini Kefalakes, Theresa Schweitzer, Segev Barak, Andreas Pich and Claudia Grothe; Final approval: Leonie Hose, Alina Katharina Langenhagen, Ekaterini Kefalakes, Theresa Schweitzer, Sabrina Kubinski, Segev Barak, Andreas Pich and Claudia Grothe.

ACKNOWLEDGEMENTS

We would like to thank Dr Dittrich-Breiholz and the Research Core Unit Genomics (RCUG) of the Hannover Medical School for their technical support and for RNA sequencing. Open Access funding enabled and organized by Projekt DEAL.

CONFLICT OF INTEREST STATEMENT

The authors declare that the research was conducted in the absence of any commercial or financial relationships that could be construed as a potential conflict of interest.

PEER REVIEW

The peer review history for this article is available at https://www.webofscience.com/api/gateway/wos/peer-review/10.1111/ejn.16234.

DATA AVAILABILITY STATEMENT

The following information was supplied regarding data availability:

Information on animals used in the alcohol drinking experiment, primer pairs used for qRT-PCR, top 10 upregulated and downregulated genes mDAergic neurons of FGF-2-KO mice, proof of principle data of selective isolation of mDAergic neurons via DAT-specific IP and data on RNA-seq quality control are available in the supplementary material.

REFERENCES

Agrawal, A., & Lynskey, M. T. (2008). Are there genetic influences on addiction: Evidence from family, adoption and twin studies. *Addiction*, *103*, 1069–1081. https://doi.org/10.1111/j.1360-0443.2008.02213.x

Anderegg, A., Poulin, J. F., & Awatramani, R. (2015). Molecular heterogeneity of midbrain dopaminergic neurons—Moving toward single cell resolution. *FEBS Letters*, *589*, 3714–3726. https://doi.org/10.1016/j.febslet.2015.10.022

Bäckman, C. M., Malik, N., Zhang, Y., Shan, L., Grinberg, A., Hoffer, B. J., Westphal, H., & Tomac, A. C. (2006). Characterization of a mouse strain expressing Cre recombinase from the 3′ untranslated region of the dopamine transporter locus. *Genesis*, *44*, 383–390. https://doi.org/10.1002/dvg.20228

Baik, J. H. (2020). Stress and the dopaminergic reward system. *Experimental & Molecular Medicine*, *52*, 1879–1890. https://doi.org/10.1038/s12276-020-00532-4

Bain, J., McLauchlan, H., Elliott, M., & Cohen, P. (2003). The specificities of protein kinase inhibitors: An update. *The Biochemical Journal*, *371*, 199–204. https://doi.org/10.1042/bj20021535

Barak, S., Wang, J., Ahmadiantehrani, S., Ben Hamida, S., Kells, A. P., Forsayeth, J., Bankiewicz, K. S., & Ron, D. (2015). Glial cell line-derived neurotrophic factor (GDNF) is an endogenous protector in the mesolimbic system against excessive alcohol consumption and relapse. *Addiction Biology*, *20*, 629–642. https://doi.org/10.1111/adb.12152

Baron, O., Ratzka, A., & Grothe, C. (2012). Fibroblast growth factor 2 regulates adequate nigrostriatal pathway formation in mice. *The Journal of Comparative Neurology*, *520*, 3949–3961. https://doi.org/10.1002/cne.23138

Beier, K. T., Steinberg, E. E., DeLoach, K. E., Xie, S., Miyamichi, K., Schwarz, L., Gao, X. J., Kremer, E. J., Malenka, R. C., & Luo, L. (2015). Circuit architecture of VTA dopamine neurons revealed by systematic input-output mapping. *Cell*, *162*, 622–634. https://doi.org/10.1016/j.cell.2015.07.015

Björklund, A., & Dunnett, S. B. (2007a). Dopamine neuron systems in the brain: An update. *Trends in Neurosciences*, *30*, 194–202. https://doi.org/10.1016/j.tins.2007.03.006

Björklund, A., & Dunnett, S. B. (2007b). Fifty years of dopamine research. *Trends in Neurosciences*, *30*, 185–187. https://doi.org/10.1016/j.tins.2007.03.004

Bodea, G. O., & Blaess, S. (2015). Establishing diversity in the dopaminergic system. *FEBS Letters*, *589*, 3773–3785. https://doi.org/10.1016/j.febslet.2015.09.016

Brischoux, F., Chakraborty, S., Brierley, D. I., & Ungless, M. A. (2009). Phasic excitation of dopamine neurons in ventral VTA by noxious stimuli. *Proceedings of the National Academy of Sciences of the United States of America*, *106*, 4894–4899. https://doi.org/10.1073/pnas.0811507106

Cardoso, T., & Lévesque, M. (2020). Toward generating subtype-specific mesencephalic dopaminergic neurons in vitro. *Frontiers in Cell and Development Biology*, *8*, 443. https://doi.org/10.3389/fcell.2020.00443

Carlsson, A., Falck, B., & Hillarp, N. A. (1962). Cellular localization of brain monoamines. *Acta Physiologica Scandinavica. Supplementum*, *56*, 1–28.

Carnicella, S., Kharazia, V., Jeanblanc, J., Janak, P. H., & Ron, D. (2008). GDNF is a fast-acting potent inhibitor of alcohol consumption and relapse. *Proceedings of the National Academy of Sciences of the United States of America*, *105*, 8114–8119. https://doi.org/10.1073/pnas.0711755105

Carnicella, S., Ron, D., & Barak, S. (2014). Intermittent ethanol access schedule in rats as a preclinical model of alcohol abuse. *Alcohol*, *48*, 243–252. https://doi.org/10.1016/j.alcohol.2014.01.006

Cox, J., & Mann, M. (2008). MaxQuant enables high peptide identification rates, individualized p.p.b.-range mass accuracies and proteome-wide protein quantification. *Nature Biotechnology*, *26*, 1367–1372. https://doi.org/10.1038/nbt.1511

Dahlstroem, A., & Fuxe, K. (1964). Evidence for the existence of monoamine-containing neurons in the central nervous system. I. Demonstration of monoamines in the cell bodies of brain stem neurons. *Acta Physiologica Scandinavica. Supplementum*, Suppl, *232*, 231–255.

Dono, R., Texido, G., Dussel, R., Ehmke, H., & Zeller, R. (1998). Impaired cerebral cortex development and blood pressure regulation in FGF-2-deficient mice. *The EMBO Journal*, *17*, 4213–4225. https://doi.org/10.1093/emboj/17.15.4213

Eswarakumar, V. P., Lax, I., & Schlessinger, J. (2005). Cellular signaling by fibroblast growth factor receptors. *Cytokine &*

Growth Factor Reviews, *16*, 139–149. https://doi.org/10.1016/j.cytogfr.2005.01.001

Even-Chen, O., & Barak, S. (2019). Inhibition of FGF receptor-1 suppresses alcohol consumption: Role of PI3 kinase signaling in dorsomedial striatum. *The Journal of Neuroscience*, *39*, 7947–7957. https://doi.org/10.1523/JNEUROSCI.0805-19.2019

Even-Chen, O., Herburg, L., Kefalakes, E., Urshansky, N., Grothe, C., & Barak, S. (2022). FGF2 is an endogenous regulator of alcohol reward and consumption. *Addiction Biology*, *27*, e13115. https://doi.org/10.1111/adb.13115

Even-Chen, O., Sadot-Sogrin, Y., Shaham, O., & Barak, S. (2017). Fibroblast growth factor 2 in the dorsomedial striatum is a novel positive regulator of alcohol consumption. *The Journal of Neuroscience*, *37*, 8742–8754. https://doi.org/10.1523/JNEUROSCI.0890-17.2017

Ford-Perriss, M., Abud, H., & Murphy, M. (2001). Fibroblast growth factors in the developing central nervous system. *Clinical and Experimental Pharmacology & Physiology*, *28*, 493–503. https://doi.org/10.1046/j.1440-1681.2001.03477.x

Garritsen, O., van Battum, E. Y., Grossouw, L. M., & Pasterkamp, R. J. (2023). Development, wiring and function of dopamine neuron subtypes. *Nature Reviews. Neuroscience*, *24*, 134–152. https://doi.org/10.1038/s41583-022-00669-3

Gómez-Pinilla, F., Vu, L., & Cotman, C. W. (1995). Regulation of astrocyte proliferation by FGF-2 and heparan sulfate in vivo. *The Journal of Neuroscience*, *15*, 2021–2029. https://doi.org/10.1523/JNEUROSCI.15-03-02021.1995

Grothe, C., & Timmer, M. (2007). The physiological and pharmacological role of basic fibroblast growth factor in the dopaminergic nigrostriatal system. *Brain Research Reviews*, *54*, 80–91. https://doi.org/10.1016/j.brainresrev.2006.12.001

Junemann, J., Lämmerhirt, C. M., Polten, F., Just, I., Gerhard, R., Genth, H., & Pich, A. (2017). Quantification of small GTPase glucosylation by clostridial glucosylating toxins using multiplexed MRM analysis. *Proteomics*, *17*, 1700016. https://doi.org/10.1002/pmic.201700016

Kamath, T., Abdulraouf, A., Burris, S. J., Langlieb, J., Gazestani, V., Nadaf, N. M., Balderrama, K., Vanderburg, C., & Macosko, E. Z. (2022). Single-cell genomic profiling of human dopamine neurons identifies a population that selectively degenerates in Parkinson's disease. *Nature Neuroscience*, *25*, 588–595. https://doi.org/10.1038/s41593-022-01061-1

Kramer, D. J., Risso, D., Kosillo, P., Ngai, J., & Bateup, H. S. (2018). Combinatorial expression of grp and Neurod6 defines dopamine neuron populations with distinct projection patterns and disease vulnerability. *eNeuro*, *5*, ENEURO.0152–ENEU18.2018. https://doi.org/10.1523/ENEURO.0152-18.2018

La Manno, G., Gyllborg, D., Codeluppi, S., Nishimura, K., Salto, C., Zeisel, A., Borm, L. E., Stott, S. R. W., Toledo, E. M., Villaescusa, J. C., Lönnerberg, P., Ryge, J., Barker, R. A., Arenas, E., & Linnarsson, S. (2016). Molecular diversity of midbrain development in mouse, human, and stem cells. *Cell*, *167*, 566–580.e519. https://doi.org/10.1016/j.cell.2016.09.027

Lammel, S., Hetzel, A., Häckel, O., Jones, I., Liss, B., & Roeper, J. (2008). Unique properties of mesoprefrontal neurons within a dual mesocorticolimbic dopamine system. *Neuron*, *57*, 760–773. https://doi.org/10.1016/j.neuron.2008.01.022

Liran, M., Rahamim, N., Ron, D., & Barak, S. (2020). *Growth factors and alcohol use disorder* (Vol. 10). Cold Spring Harb Perspect Med. https://doi.org/10.1101/cshperspect.a039271

Mähler Convenor, M., Berard, M., Feinstein, R., Gallagher, A., Illgen-Wilcke, B., Pritchett-Corning, K., & Raspa, M. (2014). FELASA recommendations for the health monitoring of mouse, rat, hamster, guinea pig and rabbit colonies in breeding and experimental units. *Laboratory Animals*, *48*, 178–192. https://doi.org/10.1177/0023677213516312

Morel, C., Montgomery, S., & Han, M. H. (2019). Nicotine and alcohol: The role of midbrain dopaminergic neurons in drug reinforcement. *The European Journal of Neuroscience*, *50*, 2180–2200. https://doi.org/10.1111/ejn.14160

Ornitz, D. M., & Itoh, N. (2022). New developments in the biology of fibroblast growth factors. *WIREs Mech Dis*, *14*, e1549. https://doi.org/10.1002/wsbm.1549

Poulin, J. F., Caronia, G., Hofer, C., Cui, Q., Helm, B., Ramakrishnan, C., Chan, C. S., Dombeck, D. A., Deisseroth, K., & Awatramani, R. (2018). Mapping projections of molecularly defined dopamine neuron subtypes using intersectional genetic approaches. *Nature Neuroscience*, *21*, 1260–1271. https://doi.org/10.1038/s41593-018-0203-4

Poulin, J. F., Gaertner, Z., Moreno-Ramos, O. A., & Awatramani, R. (2020). Classification of midbrain dopamine neurons using single-cell gene expression profiling approaches. *Trends in Neurosciences*, *43*, 155–169. https://doi.org/10.1016/j.tins.2020.01.004

Poulin, J. F., Zou, J., Drouin-Ouellet, J., Kim, K. Y., Cicchetti, F., & Awatramani, R. B. (2014). Defining midbrain dopaminergic neuron diversity by single-cell gene expression profiling. *Cell Reports*, *9*, 930–943. https://doi.org/10.1016/j.celrep.2014.10.008

Ratzka, A., Baron, O., Stachowiak, M. K., & Grothe, C. (2012). Fibroblast growth factor 2 regulates dopaminergic neuron development in vivo. *Journal of Neurochemistry*, *122*, 94–105. https://doi.org/10.1111/j.1471-4159.2012.07768.x

Reuss, B., & Unsicker, K. (2000). Survival and differentiation of dopaminergic mesencephalic neurons are promoted by dopamine-mediated induction of FGF-2 in striatal astroglial cells. *Molecular and Cellular Neurosciences*, *16*, 781–792. https://doi.org/10.1006/mcne.2000.0906

Reuss, B., & von Bohlen und Halbach, O. (2003). Fibroblast growth factors and their receptors in the central nervous system. *Cell and Tissue Research*, *313*, 139–157. https://doi.org/10.1007/s00441-003-0756-7

Roeper, J. (2013). Dissecting the diversity of midbrain dopamine neurons. *Trends in Neurosciences*, *36*, 336–342. https://doi.org/10.1016/j.tins.2013.03.003

Ron, D., & Barak, S. (2016). Molecular mechanisms underlying alcohol-drinking behaviours. *Nature Reviews. Neuroscience*, *17*, 576–591. https://doi.org/10.1038/nrn.2016.85

Root, D. H., Barker, D. J., Estrin, D. J., Miranda-Barrientos, J. A., Liu, B., Zhang, S., Wang, H. L., Vautier, F., Ramakrishnan, C., Kim, Y. S., Fenno, L., Deisseroth, K., & Morales, M. (2020). Distinct signaling by ventral tegmental area glutamate, GABA, and combinatorial glutamate-GABA neurons in motivated behavior. *Cell Reports*, *32*, 108094. https://doi.org/10.1016/j.celrep.2020.108094

Rösner, S., Hackl-Herrwerth, A., Leucht, S., Lehert, P., Vecchi, S., & Soyka, M. (2010). Acamprosate for alcohol dependence. *Cochrane Database of Systematic Reviews*, *9*, Cd004332.

Rumpel, R., Baron, O., Ratzka, A., Schröder, M. L., Hohmann, M., Effenberg, A., Claus, P., & Grothe, C. (2016). Increased innervation of forebrain targets by midbrain dopaminergic neurons in the absence of FGF-2. *Neuroscience*, *314*, 134–144. https://doi.org/10.1016/j.neuroscience.2015.11.057

Sanz, E., Yang, L., Su, T., Morris, D. R., McKnight, G. S., & Amieux, P. S. (2009). Cell-type-specific isolation of ribosome-associated mRNA from complex tissues. *Proceedings of the National Academy of Sciences of the United States of America*, *106*, 13939–13944. https://doi.org/10.1073/pnas.0907143106

Saunders, A., Macosko, E. Z., Wysoker, A., Goldman, M., Krienen, F. M., de Rivera, H., Bien, E., Baum, M., Bortolin, L., Wang, S., Goeva, A., Nemesh, J., Kamitaki, N., Brumbaugh, S., Kulp, D., & McCarroll, S. A. (2018). Molecular diversity and specializations among the cells of the adult mouse brain. *Cell*, *174*, 1015–1030.e1016. https://doi.org/10.1016/j.cell.2018.07.028

Smajić, S., Prada-Medina, C. A., Landoulsi, Z., Ghelfi, J., Delcambre, S., Dietrich, C., Jarazo, J., Henck, J., Balachandran, S., Pachchek, S., Morris, C. M., Antony, P., Timmermann, B., Sauer, S., Pereira, S. L., Schwamborn, J. C., May, P., Grünewald, A., & Spielmann, M. (2022). Single-cell sequencing of human midbrain reveals glial activation and a Parkinson-specific neuronal state. *Brain*, *145*, 964–978. https://doi.org/10.1093/brain/awab446

Tiklová, K., Björklund, Å. K., Lahti, L., Fiorenzano, A., Nolbrant, S., Gillberg, L., Volakakis, N., Yokota, C., Hilscher, M. M., Hauling, T., Holmström, F., Joodmardi, E., Nilsson, M., Parmar, M., & Perlmann, T. (2019). Single-cell RNA sequencing reveals midbrain dopamine neuron diversity emerging during mouse brain development. *Nature Communications*, *10*, 581. https://doi.org/10.1038/s41467-019-08453-1

Timmer, M., Cesnulevicius, K., Winkler, C., Kolb, J., Lipokatic-Takacs, E., Jungnickel, J., & Grothe, C. (2007). Fibroblast growth factor (FGF)-2 and FGF receptor 3 are required for the development of the substantia nigra, and FGF-2 plays a crucial role for the rescue of dopaminergic neurons after 6-hydroxydopamine lesion. *The Journal of Neuroscience*, *27*, 459–471. https://doi.org/10.1523/JNEUROSCI.4493-06.2007

Ungless, M. A., & Grace, A. A. (2012). Are you or aren't you? Challenges associated with physiologically identifying dopamine neurons. *Trends in Neurosciences*, *35*, 422–430. https://doi.org/10.1016/j.tins.2012.02.003

Wagner, J. P., Black, I. B., & DiCicco-Bloom, E. (1999). Stimulation of neonatal and adult brain neurogenesis by subcutaneous injection of basic fibroblast growth factor. *The Journal of Neuroscience*, *19*, 6006–6016. https://doi.org/10.1523/JNEUROSCI.19-14-06006.1999

Yetnikoff, L., Lavezzi, H. N., Reichard, R. A., & Zahm, D. S. (2014). An update on the connections of the ventral mesencephalic dopaminergic complex. *Neuroscience*, *282*, 23–48. https://doi.org/10.1016/j.neuroscience.2014.04.010

SUPPORTING INFORMATION

Additional supporting information can be found online in the Supporting Information section at the end of this article.

How to cite this article: Hose, L., Langenhagen, A. K., Kefalakes, E., Schweitzer, T., Kubinski, S., Barak, S., Pich, A., & Grothe, C. (2024). A dual-omics approach on the effects of fibroblast growth factor-2 (FGF-2) on ventral tegmental area dopaminergic neurons in response to alcohol consumption in mice. *European Journal of Neuroscience*, *59*(7), 1519–1535. https://doi.org/10.1111/ejn.16234